

## Optical and Structural Characterization of TiO<sub>2</sub> Nanoparticles

Md. Ashraful Islam<sup>1</sup>, Mir Julfiker Haither<sup>2</sup>, Imran Khan<sup>3</sup>, Momtazul Islam<sup>4</sup>

<sup>1</sup>Department of CSE, Jessore Science & Technology University, Jessore, Bangladesh

<sup>2,4</sup>Dept. of AECE, Islamic University, Kushtia, Bangladesh

<sup>3</sup>Department of EEE, Jessore Science & Technology University, Jessore, Bangladesh

---

**Abstract:** Nanostructured metal oxides are gradually being interesting for their remarkable properties and mechanical fields. Many methods have been used for the preparation of nanostructured metal oxides. Here we report the synthesis of TiO<sub>2</sub> nanoparticles by anodization method at the same time optical and structural characterization was also conducted. Anodization is an electrolytic passivation process used to increase the thickness of the natural oxide layer on the surface of metal parts. Anodization was carried out using a two-electrode configuration. The close packed titanium was attached to a copper rod to form the working electrode. The titanium rod was protected by a non-conductive epoxy in order to avoid being anodized in the electrolyte. A platinum sheet (2.0×1.5cm<sup>2</sup>) connected to a copper wire was used as the counter-electrode. Anodization was conducted in 0.5ml HF with (50ml distilled water) and 0.5ml glycerol in (50 ml distilled water) with potentials ranging from (3-10) V for 2 hours at room temperature. Anodization changes the microscopic texture of the surface and changes the crystal structure of the metal near the surface. Ultraviolet-Visible Spectroscopy (UV-Vis) and X-Ray Diffraction (XRD) were carried out to characterize the optical and structural properties of the synthesized samples respectively. Optical absorbance study in the photon wavelength range between 300 and 600 nm reveals that strong absorbance peak is positioned around 423 nm (2.93ev) whereas visible energy band is almost transparent for the materials. Based on X-ray Diffraction, TiO<sub>2</sub> nanoparticles grown through anodization are amorphous. Interestingly, very small nanoparticles below 5 nm, have been shown using Stokes-Einstein equation to have unusual structural disorder that can substantially modify the properties of nanoparticles.

**Keywords:** Nanoparticles, Anodization, UV-Vis Spectroscopy, X-ray Diffraction.

---

### I. INTRODUCTION

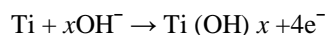
The research realms of fabrication and application of nanomaterials have attracted more scientists and engineering from various disciplines in the recent years. Nanomaterials often have novel properties which are yet to be investigated. On the other hand, our knowledge of nanoscale chemical processes for these materials is also very limited. One example is formation of nanoporous anodic metal oxides. Anodic metal oxides have diverse applications in prevention of corrosion of metal substrates from their service environment [1], forming capacitor dielectrics [2],[3], templating nanomaterials [4]-[9] and in many other fields such as catalysis, optics and electronics [10]-[13]. The best known porous anodic oxide, anodic titanium dioxide (TiO<sub>2</sub>), is now commercially available because its pores can be used as template for preparing various nanoparticles, nanowires and nanotubes. On the other hand TiO<sub>2</sub> nanoparticles have wide applications in photocatalysis, gas sensors, photoelectrolysis and photovoltaics. It has been widely accepted that the formation of the pores in anodic TiO<sub>2</sub> is based on two continuous processes, one is oxide dissolution at the electrolyte/oxide interface and the other is oxidation of metal at the oxide/metal interface. In fact, the formation mechanisms of these pores, often hexagonally ordered, are much more complicated than people normally predicted. Although the formation mechanism, pore ordering, pore size control have been extensively studied [14]-[16] and many efforts have been made to optimize the anodization conditions for these films [17]-[19], there is still much work to do in order to fully understand the electrochemical process during the anodization. Here we conducted the optical and structural studies of (TiO<sub>2</sub>) nanoparticles using UV-Vis and XRD and understanding the formation mechanism of anodic titanium dioxide (TiO<sub>2</sub>) nanoparticles.

### II. FORMATION OF NANOPARTICLES

It is widely accepted that the key processes responsible for the formation of (TiO<sub>2</sub>) nanoparticles should be:

- (1) oxide growth at the surface of the metal occurs due to an interaction of titanium with O<sup>2-</sup> or OH<sup>-</sup> anions;
- (2) Ti<sup>4+</sup> cations migrate from the oxide/metal interface to the electrolyte/oxide interface and are ejected into solution by an electric field;
- (3) field assisted dissolution of the oxide at the electrolyte/oxide interface.

Consequently, the principal chemical reaction at the hydroxide/metal interface should be:



Titanium hydroxide decomposes to form TiO<sub>2</sub> at the oxide/hydroxide interface. The overall reaction at the electrolyte/oxide interface was proposed to be:



where  $n$  was introduced to indicate the ratio of the dissociation rate of water to the dissolution rate of TiO<sub>2</sub>. Here, water dissociation and OH<sup>-</sup> ionic migration should not be ignored.

### III. EXPERIMENTAL DETAILS

It is of great technological interest to form TiO<sub>2</sub> nanoparticles from close packed titanium rod. Recently, some groups have successfully developed the technology to grow nanoparticles from titanium rod using anodization. Although the electrochemical surface process is the same as for bulk titanium foils, titanium rod may be rapidly etched away in acidic HF or neutral fluoride-containing solutions (forming soluble [TiF<sub>6</sub>]<sup>2-</sup> complexes) because the chemical dissolution rate is considerably high [20] and the quality (density, uniformity) of the titanium rod and the anodization parameters are critical to the formation process of titanium nanoparticles [21],[22]. Moreover, the electrolyte was kept at low temperatures in order to decrease the chemical dissolution rate of the oxide layer formed in acidic solution. So far, several different electrolytes have been used for producing anodic (TiO<sub>2</sub>) nanoparticles. Gong, et al. reported their anodic (TiO<sub>2</sub>) nanoparticles preparation in a 0.5 wt% HF aqueous solution at room temperature using different anodizing voltages, from 3 to 20 V [23]. It was noticed that the film thickness could not be increased further from 400-500 nm using HF-based electrolyte. Fluoride solution can help to dissolve TiO<sub>2</sub> by forming [TiF<sub>6</sub>]<sup>2-</sup> anions. However, too strong acidity of HF-solution results in a too fast dissolution of the formed TiO<sub>2</sub> nanoparticles. Mixture with other acids did not help very much, but the quality of the nanoparticles could be varied. Mor et al. reported that addition of acetic acid to a 0.5 wt% HF electrolyte in a 1:7 ratio resulted in more mechanically robust nanoparticles without changing their shape and size [24],[25]. The acidity of the electrolyte might be tuned by adding HF, H<sub>2</sub>SO<sub>4</sub> or Na<sub>2</sub>SO<sub>4</sub> in order to adjust the balance of dissociation of titanium at the electrolyte/oxide interface and oxidation of titanium at the oxide/metal interface [26],[27]. Fig. 1 shows the schematic of anodic TiO<sub>2</sub> experiment.

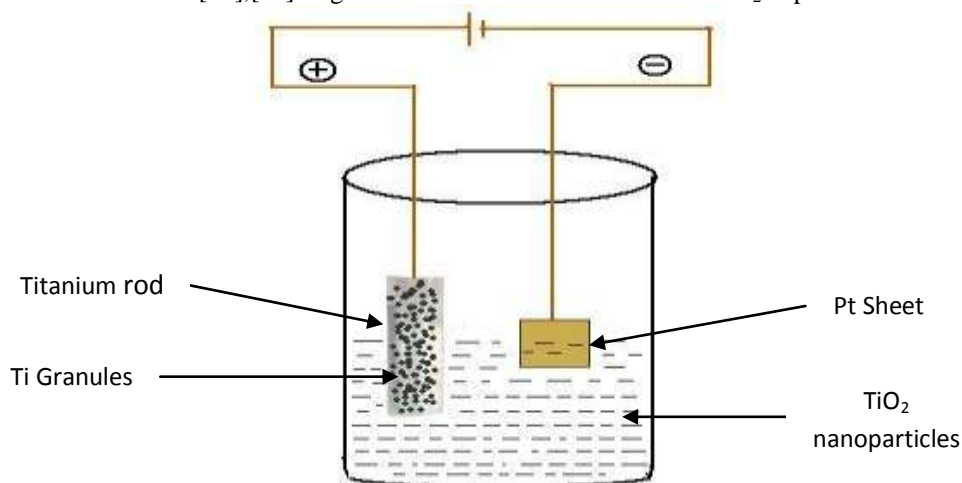


Fig. 1 The schematic of anodic TiO<sub>2</sub> experiment

It is very difficult to form Ti rod from Ti sheet because of its high melting point (1668<sup>0</sup> C). Therefore, in this work, titanium granules were packed under high pressure to form titanium rod working as an electrode and a platinum sheet (2.0×1.5 cm<sup>2</sup>) was used as the counter-electrode. It was suggested that the successfully achieving nanoparticles was to minimize water content in the anodization bath to less than 5%. As with organic electrolytes donation of oxygen is more difficult in comparison with water, thus reducing the tendency to form oxide and slowing down the process of the nanoparticles growth. At the same time, the reduction in the water content reduces the chemical dissolution of the oxide in the fluorine containing electrolytes and hence aids the nanoparticles formation. In this experiment TiO<sub>2</sub> nanoparticles was obtained by anodization using HF/glycerol electrolyte where solution containing 0.5ml HF in (50ml distilled water) and 0.5ml glycerol in (50 ml distilled water) with potentials ranging from (3-10) V for 2 hours at room temperature.

### IV. SYNTHESIS

Since Zwilling *et al* demonstrated the possibility of growing self-organized and ordered TiO<sub>2</sub> nanoparticles by anodic oxidation of titanium and its alloys [28], there have been many attempts to improve the structure and to exploit the functionality of these highly organized structures [29],[30]. In view of exploiting

specific TiO<sub>2</sub> properties, a good deal of attention has been given to applications in photovoltaic cells [31], photocatalysis [32], sensing [33] and wettability-based templates [34] due to the unique physical and chemical properties. Many approaches such as templated synthesis, hydrothermal reaction and anodic oxidation have been developed for the preparation of TiO<sub>2</sub> nanoparticles. Among them, anodic oxidation is a relatively simple technique that can be easily automated for preparing nanoparticles. Anodization was carried out using a two-electrode configuration. The experimental setup is shown in Fig. 2.



Fig. 2 An experimental setup for the synthesis of titanium dioxide (TiO<sub>2</sub>) nanoparticles by anodization

The close packed titanium was attached to a copper rod to form the working electrode. The titanium rod was protected by a non-conductive epoxy in order to avoid being anodized in the electrolyte. A platinum sheet (2.0×1.5 cm<sup>2</sup>) connected to a copper wire was used as the counter-electrode. The distance between the working and counter-electrodes was kept at 3.0 cm. A dc power source (model GPS-3030D) supplied the required anodization potential in a single step (without ramping). Anodization was conducted in 0.5ml HF with (50 ml distilled water) and 0.5 ml glycerol in (50 ml distilled water) with potentials ranging from (3-10) V for 2 hours at room temperature. Clearly, active passive transition occurred at the beginning of the experiment and then a second current increase occurred at about 3300 mV in the HF electrolyte. Such behavior is frequently observed in the aqueous fluoride-containing electrolyte for anodic pore-forming reactions that display self-organization. However, this phenomenon is not obvious in the glycerol electrolyte due to its high dielectric constants and viscosity. A low current density was found in the viscous electrolyte, which is one-tenth of the HF electrolyte. This indicates that the anodization process is controlled by diffusion and hence the dependence of the diffusion constant on the viscosity in a Stokes–Einstein manner:  $D = k_B T / 6\pi\eta r$ , where  $k_B$  is Boltzmann's constant,  $T$  is the absolute temperature,  $\eta$  is the dynamic viscosity and  $r$  is the radius of a spherical body. Therefore, a lower current density with weaker local acidification and lower chemical dissolution rate of the nanoparticles can be obtained for viscous electrolytes. During the anodization process the current rises and then drops to a minimum because of the formation of compact oxide layer. After an initial decrease, the current increases slowly for a short time as the titanium nanoparticles start to form. Then the current starts to decay again as the titanium nanoparticles become thicker and more resistive while the titanium rod below the oxide layer becomes thinner. As the last of the Ti rod is consumed, the current suddenly increases because the electrolyte, especially for aqueous solution is interacting. At this point, the sample must be quickly removed from the electrolyte to preserve the nanoparticles or else it will be consumed by the HF. The liquid sample was then mounted in the sample chamber while pure distill water was taken in the reference beam position for the optical absorption study of the sample using UV-VIS 1700 Shimadzu spectrophotometer and band gap energy was calculated from the absorbance curve. Structural studies of anodic (TiO<sub>2</sub>) nanoparticles were obtained from X-ray diffraction (XRD) Philips PW 3040 powder diffractometer using Cu K $\alpha$  radiation source.

## V. RESULTS & DISCUSSION

### 1. Optical Absorption Spectroscopy

Optical absorbance is a powerful method to determine the energy gap and particle size as well as optical properties of the samples. The optical absorbances of the nanoparticles were observed using double beam automated spectrophotometer SHIMADZU (UV-1700pc). The absorption spectrum of a semiconductor defines its possible uses. The useful semiconductors for photocatalysis have a bandgap comparable to the energy

of the photons of visible or ultraviolet light, having a value of  $E_g < 3.5$  eV. The majority of authors have determined that in TiO<sub>2</sub> the rutile has a direct band gap of 3.06 eV and an indirect one of 3.10 eV and the anatase has only an indirect band gap of 3.23 eV [35],[36]. However, Reddy's work [37] shows that a bandgap of anatase phase from the plot for indirect transition are quite low (2.95 – 2.98 eV), which led them, contrary to the other authors, to conclude that the direct transition is more favorable for TiO<sub>2</sub> nanoparticles with anatase phase. There have been reported values in the literature from 2.86 to 3.34 eV for the anatase phase.

Here in, UV–Vis absorption spectra were taken in the photon wavelength range between 300 and 600 nm. Fig. 3 shows the UV-vis absorption spectrum of electrochemically synthesized TiO<sub>2</sub> nanoparticles dissolved in distilled water. As in Fig. 2 the optical absorption peak has been found at 423 nm (2.93eV). Furthermore, the band gap energy and the diameter of TiO<sub>2</sub> nanoparticles could be obtained by applying the following equations [38]- [40].

$$(\alpha' h\nu)^n = A(h\nu - E_g) \quad (1)$$

where  $E_g$  is the absorption band gap,  $\alpha'$  is the absorption coefficient,  $h\nu$  is the photon energy,  $A$  is the absorbance and  $n$  is either 2 for a direct band gap material or  $1/2$  for indirect band gap material. When a semiconductor absorbs photons of energy larger than the gap of the semiconductor, an electron is transferred from the valence band to the conduction band where there occurs an abrupt increase in the absorbency of the material to the wavelength corresponding to the band gap energy. When, in this transition, the electron momentum is conserved, the transition is direct, but if the momentum does not conserve this transition it must be attended by a photon, this is an indirect transition [41],[42]. Using (1) and considering the value  $n=2$ , we can determine the corresponding band gap of the sample which have been found to be 2.93 eV. The band gap energy of bulk TiO<sub>2</sub> can be calculated by using the following equation:

$$E = E_{bulk} + \frac{h^2 \pi^2}{2R^2} \left[ \frac{1}{m_e} + \frac{1}{m_h} \right] - \frac{1.786e^2}{\epsilon R} \quad (2)$$

where  $E$  is the band-gap energy of the nanoparticle as determined from the UV–VIS absorbance spectrum;  $E_{bulk}$  is the band-gap energy of bulk TiO<sub>2</sub> at room temperature,  $h$  is Planck's constant,  $R$  is the particle radius,  $m_e$  is the effective mass of conduction-band electron in TiO<sub>2</sub>,  $m_h$  is the effective mass of valence-band hole in TiO<sub>2</sub>;  $e$  is the elementary charge,  $\epsilon$  is the relative permittivity of TiO<sub>2</sub>. A derivation of this equation is presented elsewhere [43],[44]. The band gap of nanoparticles can be calculated using the cutoff wavelength obtained from the absorbance spectrum of a TiO<sub>2</sub> nanoparticles.

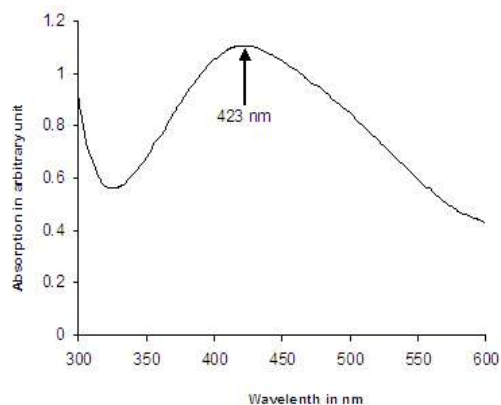


Fig. 3 Optical absorption spectra of TiO<sub>2</sub> nanoparticles in the photon wavelength range between 300 and 600 nm

Here it is also observed that TiO<sub>2</sub> nanoparticles is transparent in visible region and shows almost sharp absorbance peak around 2.93 eV. The value  $n=1/2$  does not produce any meaningful data for the band gap energy which corresponds that TiO<sub>2</sub> is a direct band gap type semiconductor.

## 2. X-Ray Diffraction Study

XRD is a very important experimental technique that has been used to address all issues related to the crystal structure of solids, including lattice constants and geometry identification of unknown materials. The X-ray diffraction (XRD) patterns for titanium dioxide samples were recorded on a SHIMADZU-6000<sub>PC</sub> X-ray powder diffractometer with Cu K $\alpha$  radiation (Cu K $\alpha$ :  $\lambda = 1.5406$  Å) with  $2\theta$  ranging from  $10^\circ$  to  $80^\circ$  at the speed of  $2^\circ\text{min}^{-1}$ . The samples were deposited on the glass substrates. Based on X-ray Diffraction, nanoparticles grown through anodization are amorphous [45]. Fig. 4 shows and proves that the XRD of the synthesized TiO<sub>2</sub> nanoparticles through anodization in an electrolytic solution is amorphous.

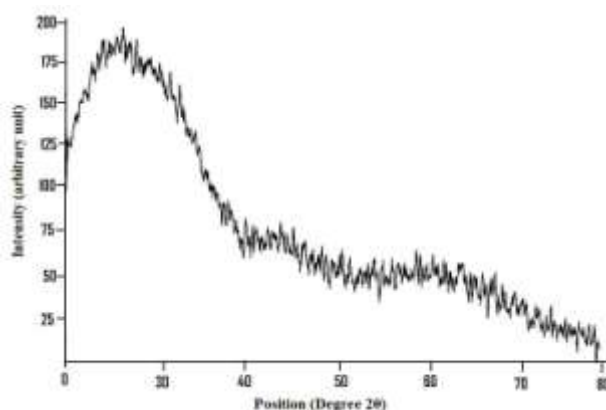


Fig. 4 XRD patterns of amorphous TiO<sub>2</sub> synthesized by anodization method

There are some important causes for a synthesized TiO<sub>2</sub> nanoparticles through anodization is amorphous. However, some researchers have different opinions. Macak et al. suggested that oxide dissolution in the growth of anodic titanium dioxide was a dominant factor rather than the electric field aided ion transportation. As the dissolution rate of titanium dioxide greatly depend on the local acidity in an F-containing electrolyte, the pores grow at the higher acidic pore bottom rather than the low acidic pore mouth [46]-[48]. This method cannot explain the regular shape and ordering of the pores at an early stage. It is even more difficult to elucidate the formation of the gap between the nanoparticles using this method. Therefore, the XRD report using this method is amorphous. In Fig. 4, a decreasing of the peak intensity of the anatase phase in materials with quantities of water below the stoichiometric ratio ( $R_{1(\text{water/Ti})} = 5$  and  $R_{2(\text{HF/Ti})} = 0.1$ ) was observed and an amorphous material was obtained due to limited hydrolysis of the titanium precursor. Interestingly, very small nanoparticles, below 5 nm using Stokes-Einstein equation have been shown to have unusual structural disorder that can substantially modify the properties of nanoparticles.[49],[50] Using a combination of small-angle and high energy wide-angle X-ray scattering measurements, Gilbert et al. investigated interior strain and disorder of nanoparticles directly using real-space pair distribution function analysis. For spherical particles, the measured diameters from different instruments can be related because no corrections need to be made for shape. But for nonspherical particles or agglomerates and aggregates that are irregularly shaped the difference in measurements creates a need to define a volume equivalent diameter,  $D_{ve}$ , which is defined as the volume of sphere with the same volume as a particle with an irregular shape. The relationship between  $D_{ve}$  and  $D_m$  is given by-

$$D_{ve} = D_m \frac{C_s(D_{ve})}{\chi C_s(D_m)} \quad (3)$$

where  $\chi$  is the dynamic shape factor, and  $C_s(D_m)$  and  $C_s(D_{ve})$  are the Cunningham slip factors for the mobility and volume equivalent diameters, respectively. For spherical particles, the dynamic shape factor,  $\chi$  is equal to one, and the volume equivalent diameter ( $D_{ve}$ ) is equal to the measured mobility diameter ( $D_m$ ). The shape factor is typically determined from the relationship between aerodynamic diameter,  $D_a$ , and mobility diameter:

$$D_m = D_a \chi^{3/2} \sqrt{\frac{\rho_0 C_s(D_m) \sqrt{C_s(D_a)}}{\rho_p C_s(D_{ve})^{3/2}}} \quad (4)$$

where  $\rho_0$  is the reference density ( $1 \text{ g cm}^{-3}$ ),  $\rho_p$  is the density of the particle, and  $C_s(D_a)$  is the Cunningham slip factor for aerodynamic diameter and other quantities as defined above. For spherical particles the dynamic shape factor,  $\chi$ , is equal to one, and the volume equivalent diameter ( $D_{ve}$ ) is equal to the measured mobility diameter ( $D_m$ ) and the  $D_a$  is related to  $D_m$  through density.

## VI. CONCLUSION

The synthesis of TiO<sub>2</sub> nanoparticles by anodization method was first conducted then the optical characterization and structural characterization were done. Anodization changes the microscopic texture of the surface and changes the crystal structure of the metal near the surface. UV-Vis, XRD were carried out to characterize the optical and structural properties of the synthesized samples. Optical absorbance study reveals that strong absorbance peak is positioned around 423 nm (2.93eV). For the visible energy band it is almost transparent for this material. Based on X-ray Diffraction it is clear that TiO<sub>2</sub> nanoparticles grown through anodization are amorphous.

TiO<sub>2</sub> is an interesting material and there is much more scope for further work as far as TiO<sub>2</sub> nanoparticles has been investigated extensively. The hydroxide layer and surface ridges in anodic TiO<sub>2</sub> may be useful in improving the quality of the anodic TiO<sub>2</sub> nanoparticles. As mentioned in the present review, there are still many unsolved problems, e.g. refinement of the anodization conditions, confirmation of the formation mechanism, theoretical study and more accurate calculation of the water dissociation on oxide surface under a electric field, control of the pore size and porosity, full crystallization of anodic TiO<sub>2</sub> nanoparticles and discovery of more applications of the porous anodic metal oxides, etc. It is even more difficult to elucidate the formation of the gap between the nanoparticles using this method. Another area which can be further exploited is the study of the optical properties of nanocrystalline TiO<sub>2</sub>. So far, there have been very few reports on the optical properties of nanocrystalline TiO<sub>2</sub>. SEM, photoluminescence studies and non linear optical studies of nanocrystalline TiO<sub>2</sub> at low temperature is another area where further work is possible and much useful and interesting results can be obtained.

## REFERENCES

- [1] Bengough GD, Stuart JM. Brit. *Patent* 223994, 1923.
- [2] Jason AC, Wood JL. "Some electrical effects of the adsorption of water vapour by anodized aluminium", *Proc Phys Soc B* 1955; 68(12):1105-16.
- [3] Dell'Oka CJ, Pulfrey DL, Young L. *Physics of thin films*. Vol 6, Ed Francombe MH, Hoffman RW (New York: Academic) 1971,1-79.
- [4] Nakao M, Oku S, Tamamura T, et al. "GaAs and InP nanohole arrays fabricated by reactive beam etching using highly ordered alumina membrane", *Jpn J Appl Phys* 1999; 38(2B):1052-5.
- [5] Liang J, Chik H, Yun A, et al. "Two-dimensional lateral superlattice of nanostructures: nonlithographic formation by anodic membrane template", *J Appl Phys* 2002; 91(4): 2544-6.
- [6] Chen L, Yin AJ, Im JS, et al. "Fabrication of 50–100 nm patterned InGaN blue light emitting heterostructures", *Phys Stat Sol A* 2001; 188(1):135-8.
- [7] Li J, Papadopoulos C, Xu JM. "Highly-ordered carbon nanotube arrays for electronics applications", *Appl Phys Lett* 1999; 75(3):367-9.
- [8] Li J, Papadopoulos C, Xu J. "Growing Y-junction carbon nanotubes", *Nature* 1999; 402(6759):253-4.
- [9] Hu W, Gong D, Chen Z, et al. "Growth of well-aligned carbon nanotube arrays on silicon substrates using porous alumina film as a nanotemplate", *Appl Phys Lett* 2001; 79(19):3083-5.
- [10] Basu S, Chatterjee S, Saha M, et al. "Study of electrical characteristics of porous alumina sensors for detection of low moisture in gases", *Sens and Actuat B: Chemical* 2001; 79(2):182-6.
- [11] Yang BC, Uchida M, Kim HM, et al. "Preparation of bioactive titanium metal via anodic oxidation treatment", *Biomaterials* 2004; 25(6):1003–10.
- [12] Mor GK, Shankar K, Paulose M, et al. "Enhanced photocleavage of water using titania nanotube arrays", *Nano Lett* 2005; 5(1):191-5.
- [13] Mor G.K, Shankar K, Paulose M, et al. "Use of highly-ordered TiO<sub>2</sub> nanotube arrays in dye- sensitized solar cells", *Nano Lett* 2006; 6(2):215-8.
- [14] Hoar TP, Mott NF. "A mechanism for the formation of porous anodic oxide films aluminium", *J Phys Chem Solids* 1959; 9(2):97-9.
- [15] Heber KV. "Studies on porous Al<sub>2</sub>O<sub>3</sub> growth-I. Physical model", *Electrochim Acta* 1978; 23(2):127-33.
- [16] Thompson GE, Wood GC. Anodic films on aluminium. In treatise on materials science and technology, Vol. 23: Corrosion: Aqueous Process and Passive Films; Scully, J. C., Ed.; Academic Press Inc.: New York, 1983; Chapter 5, 205-329.
- [17] Masuda H, Fukuda K. "Ordered metal nanohole arrays made by a two-step replication of honeycomb structures of anodic alumina", *Science* 1995;268(9):1466-8.
- [18] Masuda H, Yosuya M, Ishida M. "Spatially selective metal deposition into a pore-array structure of anodic porous alumina using a microelectrode", *Jpn J Appl Phys* 1998; 37(9A/B):1090-2.
- [19] Macak JM, Tsuchiya H, Taveira L, et al. "Smooth anodic TiO<sub>2</sub> nanotubes", *Angew Chem Int Ed* 2005; 44(45):7463-5.
- [20] Macak J M, Tsuchiya H, Berger S, Bauer S, Fujimoto S and Schmuki P 2006 *Chem. Phys. Lett.* **428** 421
- [21] Mor G K, Varghese O K, Paulose M and Grimes C A 2005 *Adv. Funct. Mater.* **15** 1291
- [22] Paulose M, Shankar K, Varghese O K, Mor G K and Grimes C A 2006 *J. Phys.D: Appl. Phys.* **39** 2498
- [23] Gong DW, Grimes CA, Varghese OK, et al. "Titanium oxide nanotube arrays prepared by anodic oxidation", *J Mater Res* 2001; 16(12):3331-4.
- [24] Mor GK, Carvalho MA, Varghese OK, et al. "A room-temperature TiO<sub>2</sub>-nanotube hydrogen sensor able to self-clean photoactively from environmental contamination", *J Mater Res* 2004; 19(2):628-34.
- [25] Mor GK, Varghese OK, Paulose M, et al. "A self-cleaning, room-temperature titania-nanotube hydrogen gas sensor", *Sensor Lett* 2003; 1(1): 42-6.
- [26] Beranek R, Hildebrand H, Schmuki P. "Self-organized porous titanium oxide prepared in H<sub>2</sub>SO<sub>4</sub>/HF electrolytes", *Electrochem Solid-State Lett* 2003; 6(3): B12-4.
- [27] Macak JM, Sirotna K, Schmuki P. "Self-organized porous titanium oxide prepared in Na<sub>2</sub>SO<sub>4</sub>/NaF electrolytes", *Electrochim Acta* 2005;50(18):3679-84.
- [28] Zwilling V, Aucouturier M and Darque-Ceretti E 1999 *Electrochim. Acta* **45** 921
- [29] Gong D, Grimes C A, Varghese O K, Hu W C, Singh R S, Chen Z and Dickey E C 2001 *J. Mater. Res.* **16** 3331
- [30] Beranek R, Hildebrand H and Schmuki P 2003 *Electrochem. Solid State. Lett.* **6** B12
- [31] Mor G K, Shankar K, Paulose M, Varghese O K and Grimes C A 2006 *Nano Lett.* **6** 215
- [32] Sohn Y S, Smith Y R, Misra M and Subramanian V 2008 *Appl. Catal. B: Environ.* **84** 372
- [33] Varghese O K, Gong D W, Paulose M, Ong K G and Grimes C A 2003 *Sensors Actuators B* **93** 338
- [34] Lai Y K, Huang J Y, Gong J J, Huang Y X, Wang C L, Chen Z and Lin C J 2009 *J. Electrochem. Soc.* **156** D480
- [35] Welte A, Waldauf C, Brabec C, Wellmann P. "Application of optical for the investigation of electronic and structural properties of sol-gel processed TiO<sub>2</sub> films", *Thin Solid Films* 2008; 516: 7256-9.

- [36] Monllor-Satoca D, Gomez R, González-Hidalgo M, Salvador P. The “Diret-Indirect model: An Alternative kinetic approach in heterogeneous photocatalysis based on the degree of interaction of dissolved pollutant species with the semiconductor surface”, *Catal Today* 2007; 129: 247-55.
- [37] Reddy K, Manorama S, Redd A. “Bandgap studies on anatase titanium dioxide nanoparticles”, *Mater Chem Phys* 2002; 78: 239-45.
- [38] Nag BR, Physics of quantum well devices. *Kluwer Academic Publishers, Dordrecht*, 2000, pp 105
- [39] Brus LE, “Electron-electron and electron-hole interactions in small semiconductor crystallites: the size dependence of the lowest excited electronic state”, *J Chem Phys* 80, (1984) 4403–4409.
- [40] Bawendi MG, Steigerwald ML, Brus LE, “The quantum mechanics of larger semiconductor clusters (“quantum dots”)", *Annu Rev Phys Chem* 41, (1990) 477–496
- [41] Willardson R, Beer A. Optical Properties of III-V Compounds. *Academic Press New York* 1967; pp. 318-400.
- [42] Dressel M, Gruner G. Electrodynamics of Solids Optical Properties of Electron in Matter. *Cambridge University Press* 2002; pp. 159-65.
- [43] Kippeny, Tadd; Swafford, Laura A.; Rosenthal, Sandra J. *J Chem. Educ.* (2002), 79, 1094–1100.
- [44] Nedeljkovic, J. M.; Patel, R. C.; Kaufman, P.; Joyce-Pruden,
- [45] D. Gong et al., “Titanium oxide nanotube arrays prepared by anodic oxidation”, *Journal of Materials Research*, vol. 16, no. 12, pp. 3331–3334, 2001.
- [46] Macak JM, Tsuchiya H, Schmuki P. “High-aspect-ratio TiO<sub>2</sub> nanotubes by anodization of titanium”, *Angew Chem Int Ed* 2005; 44(14):2100-2.
- [47] Macak JM, Tsuchiya H, Taveira L, et al. “Smooth anodic TiO<sub>2</sub> nanotubes”, *Angew Chem Int Ed* 2005;44(45):7463-5.
- [48] Taveira LV, Macák JM, Tsuchiya H, et al. “Initiation and growth of self-organized TiO<sub>2</sub> nanotubes anodically formed in NH<sub>4</sub>F/(NH<sub>4</sub>)<sub>2</sub>SO<sub>4</sub> electrolytes”, *J Electrochem Soc* 2005;152(10):B 405-10.
- [49] Gilbert, B.; Huang, F.; Zhang, H. Z.; Waychunas, G. A.; Banfield, J. F. *Science* 2004, 305, 651.
- [50] Gilbert, B.; Huang, F.; Lin, Z.; Goodell, C.; Zhang, H. Z.; Banfield, J. F. *Nano Lett.* 2006, 6, 651.